Astron. Astrophys. 155, 185–192 (1986)

ASTRONOMY AND ASTROPHYSICS

Multifrequency radio continuum observations of extended galatic objects

I. Nine objects from the 2695 MHz Effelsberg galactic plane survey

W. Reich[1], E. Fürst[1], P. Reich[1], Y. Sofue[2], and T. Handa[2]

[1] Max-Planck-Institut für Radioastronomie, Auf dem Hügel 69, D-5300 Bonn 1, Federal Republic of Germany
[2] Nobeyama Radio Observatory*, Tokyo Astronomical Observatory, University of Tokyo, Minamisaku, Nagano 384-13, Japan

Received July 8, accepted September 19, 1985

Summary. The recently published 2696 MHz galactic plane survey with the Effelsberg 100-m telescope has been inspected for extended, unidentified objects. Nine of these objects have subsequently been observed at 1420, 4750 MHz and 10 GHz. Based on the available continuum radio data, we propose the following most likely identifications: two supernova remnants, five H II-regions, one radio galaxy and one object resovled into an H II-region seen in front of a supernova remnant.

Key words: radio continuum emission – supernova remnants – H II-regions

1. Introduction

In a series of papers we will present a number of extended galactic emission features, for which new high sensitive multifrequency radio continuum observations have been made. Some of these objects have been detected in the Effelsberg 2695 MHz galactic plane survey (Reich et al., 1984a). Supplementary radio data are provided by the galactic plane surveys at 1420 MHz (Kallas and Reich, 1980; Reich et al., 1986) with the 100-m telescope and at 10 GHz with the 45-m telescope of the Nobeyama Radio Observatory (Sofue et al., 1984). Several observations at 10 GHz using the same instrument have been carried out for the majority of objects in order to increase the sensitivity. Frequently, additional observations including linear polarization have been made at 4750 MHz with the 100-m telescope for some of the sources. Based on the polarization and spectral index information the nature of many objects could be determined.

A few new objects have already been reported by Reich and Fürst (1984), Reich et al. (1984b) and by Sofue et al. (1985). A giant radio galaxy has been found by Seiradakis et al. (1985), and a nonthermal diffuse object perhaps originating in a binary system has been detected by Fürst et al. (1985).

In this first paper we have selected nine objects, which have been investigated thoroughly by means of their radio emission.

In Sect. 2 we shortly refer to the method of observations, which will be the same in subsequent papers. The observational results and a short discussion of the individual sources are presented in Sect. 3.

Send offprint requests to: W. Reich

* NRO, a branch of the Tokyo Astronomical Observatory, is a facility open for the general use by researchers in the field of astronomy and astrophysics

2. Observations

Observations and the data reduction of the galactic plane surveys at 2695 MHz and 10 GHz have been described by Reich et al. (1984a) and by Sofue et al. (1984) respectively. In some cases polarization information at 2695 MHz has been obtained from the survey data (Junkes, 1985). The 1420 MHz survey has been carried out similarly as the 2695 MHz survey. At 4750 MHz we made use of the three channel receiver in the secondary focus of the 100-m telescope. At this frequency we obtained the highest angular resolution (HPBW = 2.'4) combined with high sensitive linear polarization measurements. Some relevant observational parameters are listed in Table 1.

The additional observations at 4750 MHz and 10 GHz have been made by scanning each object at least two times in orthogonal directions. The data reduction is based on the NOD2 map making procedure (Haslam, 1974). The procedures of the baselevel improvements and combinations of the individual coverages have been summarized by Reich (1984) and Wielebinski (1984). Corresponding fields have been selected from the survey data. The galactic background radiation has been subtracted to give a new relative zero-level. In some cases the estimate of the flux density suffers from insufficient accuracy of this method, in particular in cases for which sources are heavily confused by strong background emission.

The flux densities of the sources have been obtained by integrating in concentric rings beginning at the field centre. The results are listed in Table 2, contour maps and spectra are displayed in Figs. 1 to 9. In order to investigate the influence of distortion by remaining background emission, differential spectral index plots (*TT*-plots) have been performed for 2695 MHz/4750 MHz and/or for 2695 MHz/10 GHz maps respectively depending on the quality of the maps. The results are included in Table 2. A comparison with the integrated flux density spectral indices provides an indication concerning the degree of distortion by background confusion. Spectral index maps have also been made and are discussed in Sect. 3 for the individual objects.

The linear polarization observed at 4750 MHz has also been integrated and the average percentage polarization is included in Table 2.

3. Results

Maps at 1420 MHz and 2695 MHz of all sources are included in the survey data and can be found in the papers by Reich et al. (1984a, 1986). Contour plots at the highest available angular

Table 1. Observational parameters

Frequency (GHz)	1.42	2.695	4.75	10
Telescope	Effelsberg 100 m	Effelsberg 100 m	Effelsberg 100 m	Nobeyama 45 m
HPBW (arcmin)	9.3	4.27	2.4	2.7
System temperature (K)	45	60	65	100
Bandwidth (MHz)	40	80 (50)	500	1500
T_B [K][a]/S[Jy]	2	2.51	2.66	0.5
Main calibrator	3C286 14.4 Jy	3C286 10.4 Jy	3C286 7.5 Jy	NGC7027 6.4 Jy
Degree of linear polarization (%)	–	9.9	11.5	–
Polarization angle (°)	–	33	33	–

[a] Main beam brightness temperature

Table 2. Source parameters. *Note*: α_1: spectral index from integrated flux density, $S_\nu = \nu^\alpha$; α_2: spectral index from *TT*-plot 2695 MHz versus 4750 MHz; α_3: spectral index from *TT*-plot 2695 MHz versus 10 GHz

Source Name	Flux density (Jy)				Polarization at 4750 MHz (%)	Flux density spectral index			Comments
	1420 MHz	2695 MHz	4750 MHz	10 GHz		α_1	α_2	α_3	
G 7.45+0.7	4.7±1.0	5.1±0.8	5.5±0.5	–	< 3	0.14	−0.1	–	H II
G16.85−1.05	5.3±1.1	6.4±0.7	7.4±1.2	7.6±0.8	15	0.16	0.32	−0.24	Complex: SNR+H II
G30.7+1.0	5.1±0.7	4.1±0.6	3.4±0.4	2.7±0.5	32	−0.34	−0.46	–	SNR
G43.45+0.5	3.6±1.2	3.8±1.1	3.5±1.1	>1.8	< 1	0.0	−0.33	–	Radio galaxy?
G52.0+0.6	20.9±2.0	16.6±1.6	–	16.6±1.6	–	−0.09	–	−0.03	Complex H II
G55.6+0.7	2.2±0.3	1.8±0.2	1.8±0.2	1.8±0.3	< 5	−0.05	0.0	–	H II
G61.7+0.9	1.9±0.2	2.5±0.2	2.5±0.2	2.5±0.4	< 1	0.0[a]	0.0	0.0	H II
G73.9+0.9	8.0±0.8	7.9±0.8	6.7±0.5	5.4±0.5	6.3	−0.21	−0.41	–	SNR
G75.4−0.6	7.5±2.0	5.9±1.5	–	6.2±0.8	–	−0.07	–	−0.1	H II

[a] Beyond 2695 MHz

resolution and integrated spectra are shown in Figs. 1 to 9. Except for two cases the 4750 MHz observations are presented (HPBW = 2.'4). G52.0+0.6 and G75.4−0.6 have not been observed at 4750 MHz. Therefore 10 GHz maps are shown, G75.4−0.6 convolved to 4.'4 to increase the sensitivity. Flux density values of compact sources of 2695 MHz and 10 GHz are listed in the survey papers by Reich et al. (1984a) and by Sofue et al. (1984).

3.1. G7.45+0.7 ($\alpha_{50} = 17^h56^m.7$, $\delta_{50} = -22°10'$)

The integrated spectrum of this source suggests a thermal origin for the emission. No linear polarization has been found at 4750 MHz. While strong infrared emission can be seen on a photographic enlargement of the IRAS galactic plane survey (review of Henbest and Knapp, 1984), no related optical emission has been detected on the Palomar prints. According to the available data an identification of G7.45+0.7 as an H II-region is most likely. The pulsar PSR1756-22 is located in the direction of G7.45+0.7 at the position of the cross in Fig. 1a. However, in view of the suggested nature of G7.45+0.7 a physical association is unlikely.

3.2. G16.85−1.05 ($\alpha_{50} = 18^h22^m.5$, $\delta_{50} = -14°48'$)

This object has a complex structure. The H II-region RCW 164 (Rodgers et al., 1960), S50 (Sharpless, 1959) is located at the peak position (0.4 Jy/beam at 4750 MHz) of this object. The optical size quoted by Rodgers et al. (8' × 6') is in good agreement with the radio dimension of the central component. The size of S50 is reported to be about 20' corresponding to the overall size of the radio structure. However, the diffuse emission surrounding the central component is strongly polarized at 4750 MHz (up to 40%). The polarized intensity decreases in the direction of the central peak. This indicates depolarization caused by the H II-region. At 2695 MHz the integrated polarization percentage is 1.7±0.7%. This also indicates strong Faraday rotation which is not unusual in this direction towards the inner part of the Milky Way. The spectral index of the polarized emission could not be obtained, because of the large uncertainty of the baselevel subtracted in this very confused area. However, the polarization data show that G16.85−1.05 is an H II-region in front of the non-thermal emission, possibly a supernova remnant. The inverted integrated spectrum suggests the existence of an optical thick thermal component in RCW 164. The distance to RCW 164 is not

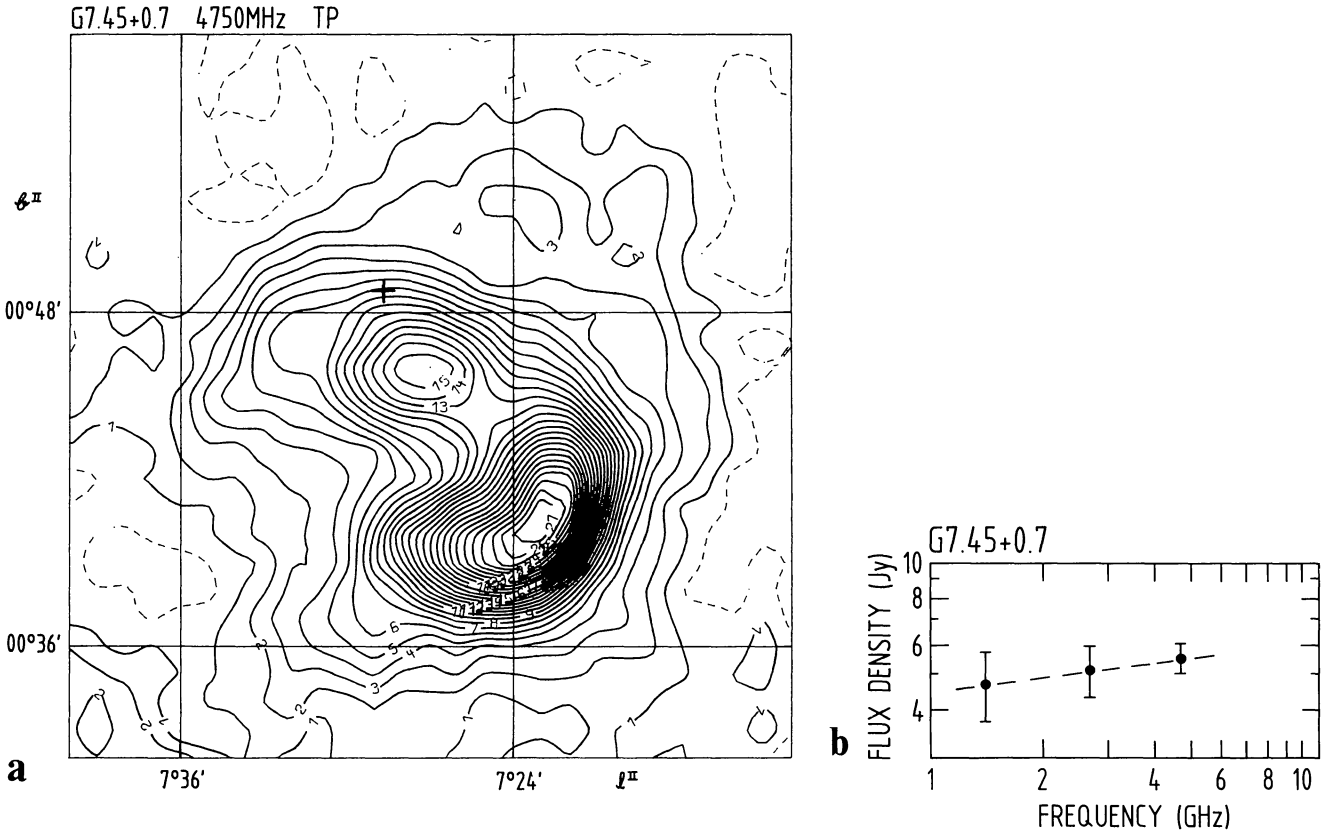

Fig. 1. a Contour plot and **b** spectrum of G7.45 + 0.7. Contour steps are in 40 mK T_B. The HPBW is 2'.4 and the r.m.s. noise is about 10 mK T_B in total power. A cross marks the position of the pulsar PSR 1756-22

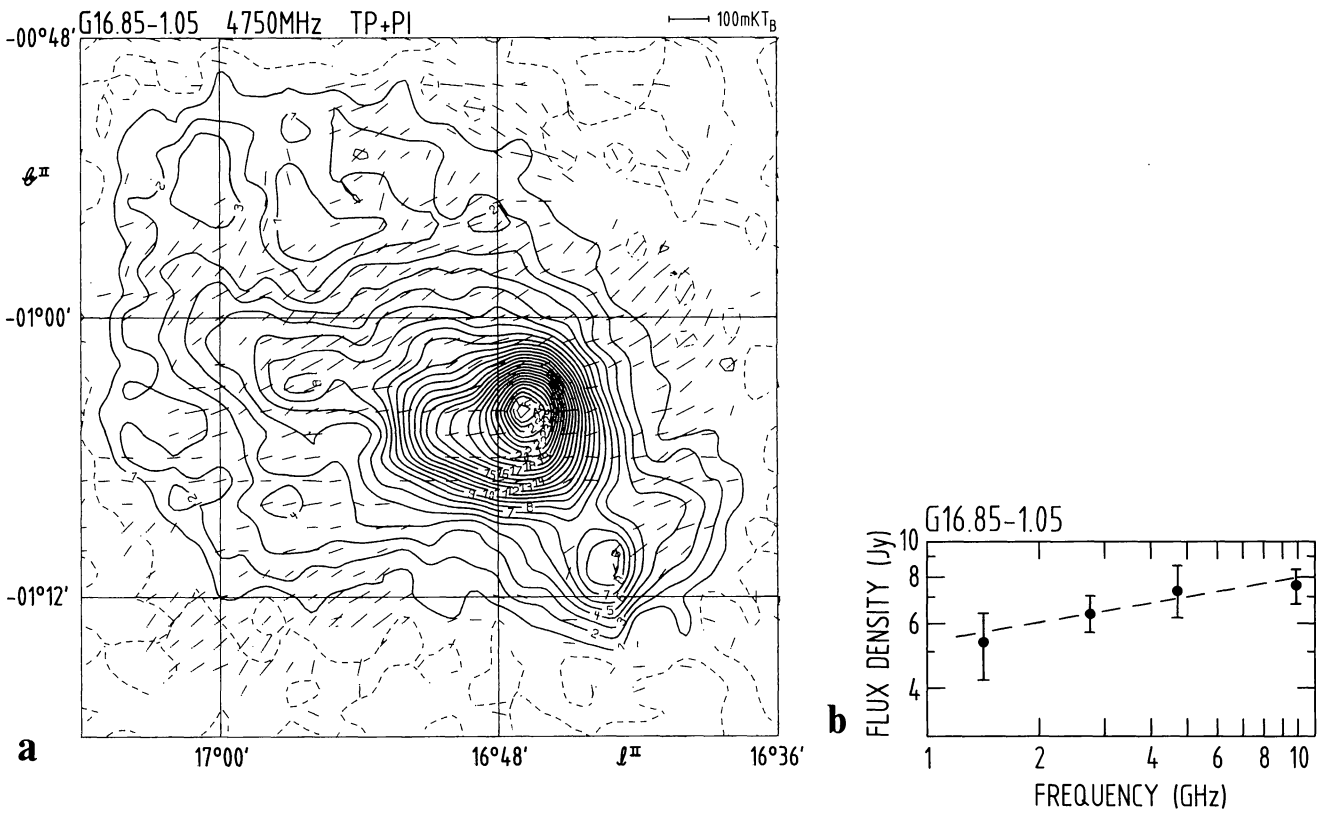

Fig. 2. a Contour plot and **b** spectrum of G16.85 − 1.05. Contour steps are in 50 mK T_B. The HPBW is 2'.4. The r.m.s. noise is about 20 mK T_B in total power and in polarized intensity (PI). PI is plotted above 40 mK T_B

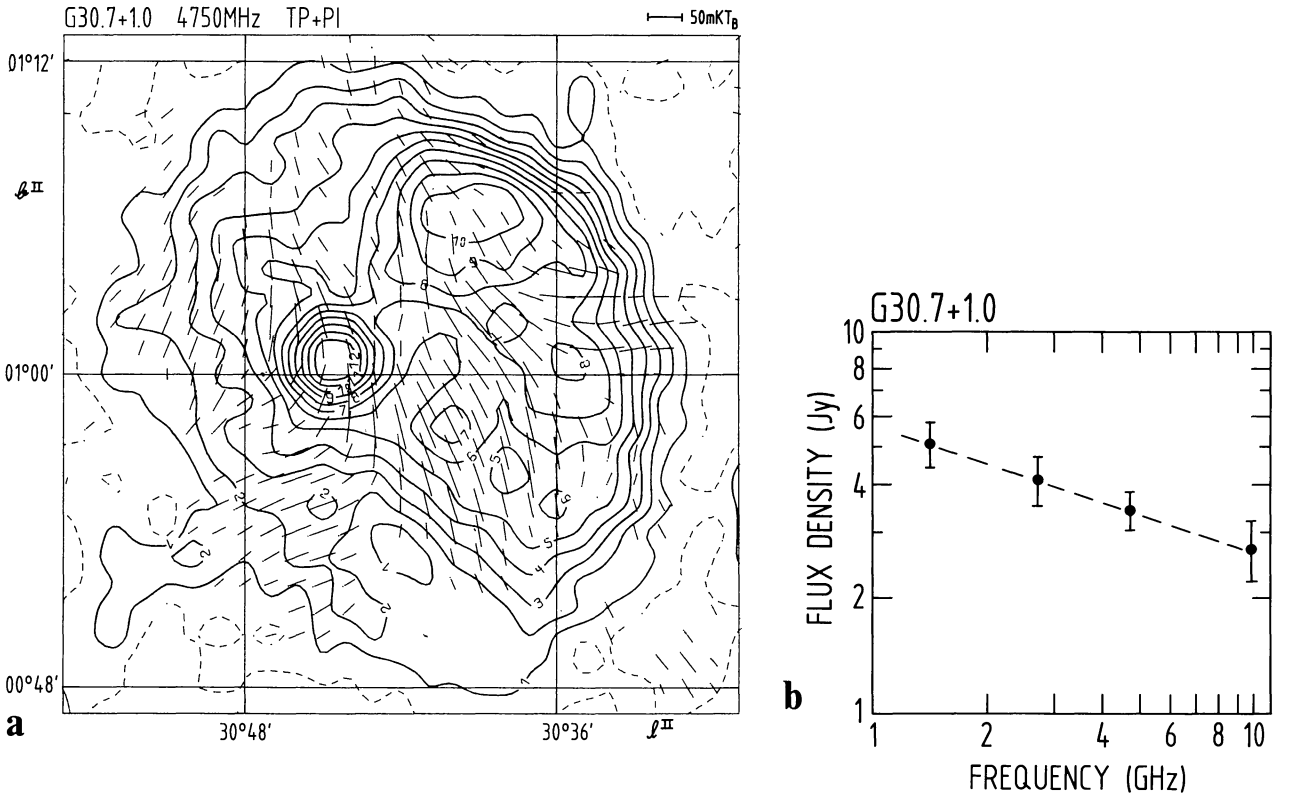

Fig. 3. **a** Contour plot and **b** spectrum of G30.7+1.0. Contour steps are in 30 mK T_B. The HPBW is 2'.4. The r.m.s. noise is about 14 mK T_B in toal power and 10 mK T_B in PI. PI is plotted above 20 mK T_B

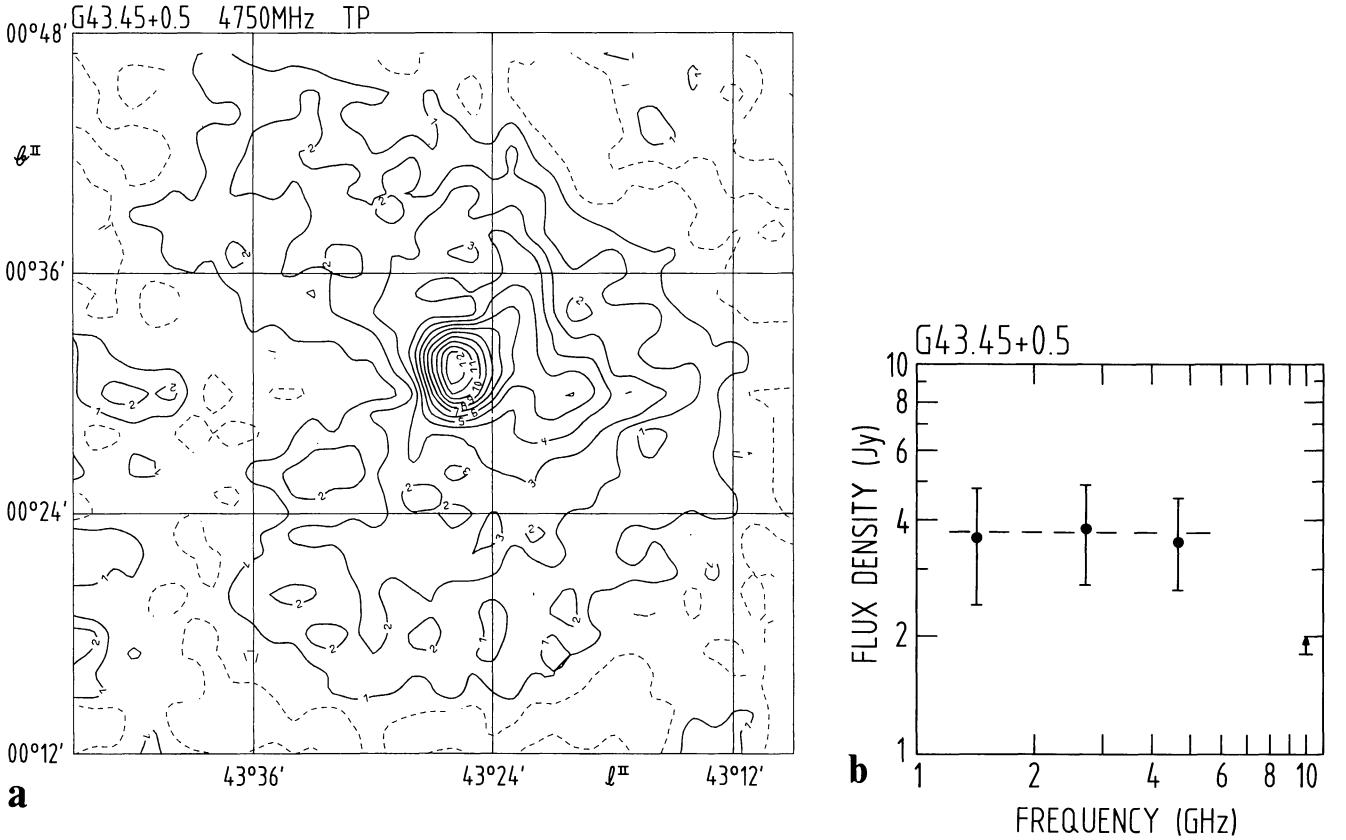

Fig. 4. **a** Contour plot and **b** spectrum of G43.45+0.5. Contour steps are in 40 mK T_B. The HPBW is 2'.4. The r.m.s. noise is about 18 mK T_B in total power

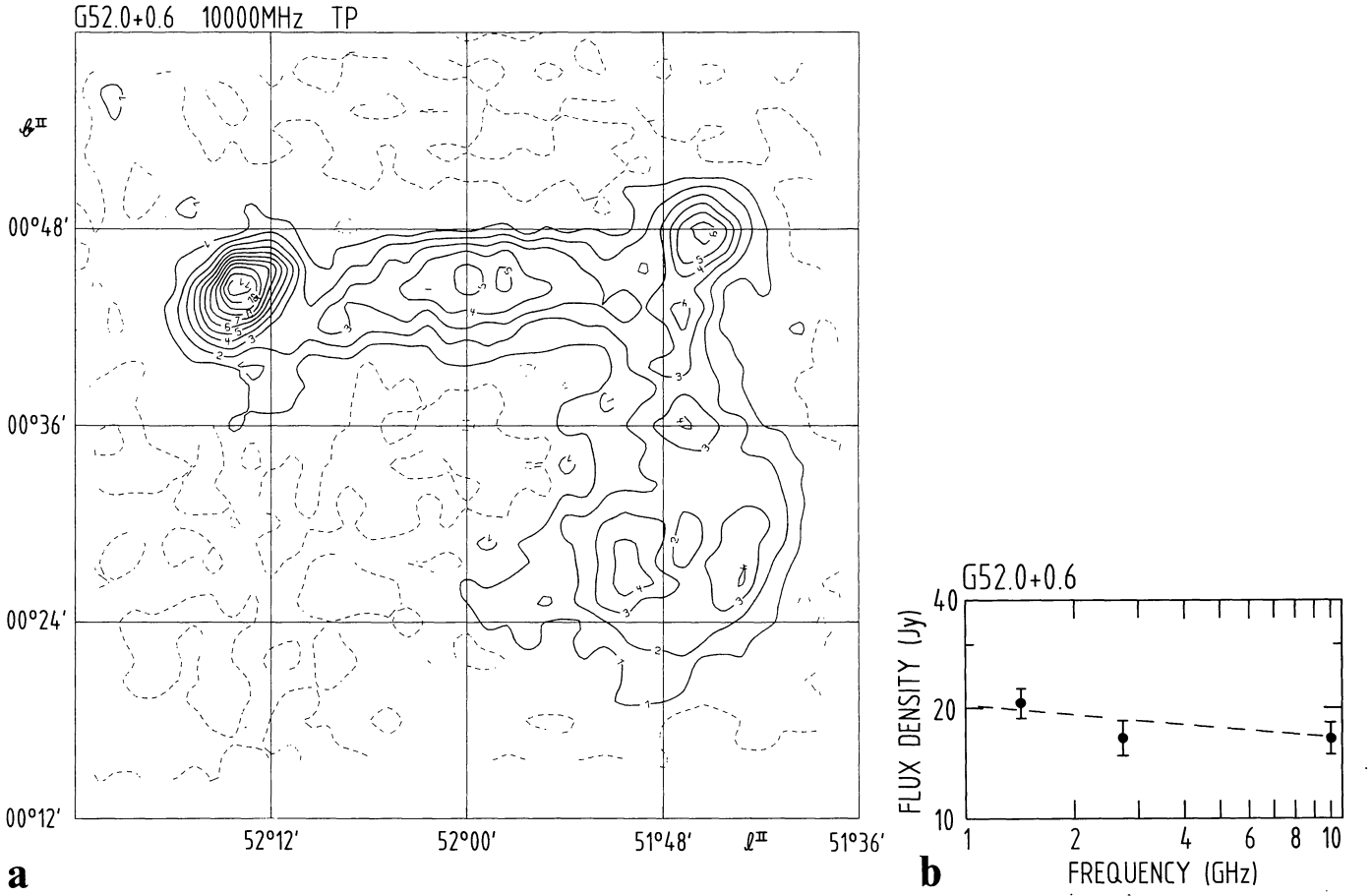

Fig. 5. **a** Contour plot and **b** spectrum of G52.0+0.6. Contour steps are in 30 mK T_B. The HPBW is 2'.7. The r.m.s. noise is about 9 mK T_B in total power

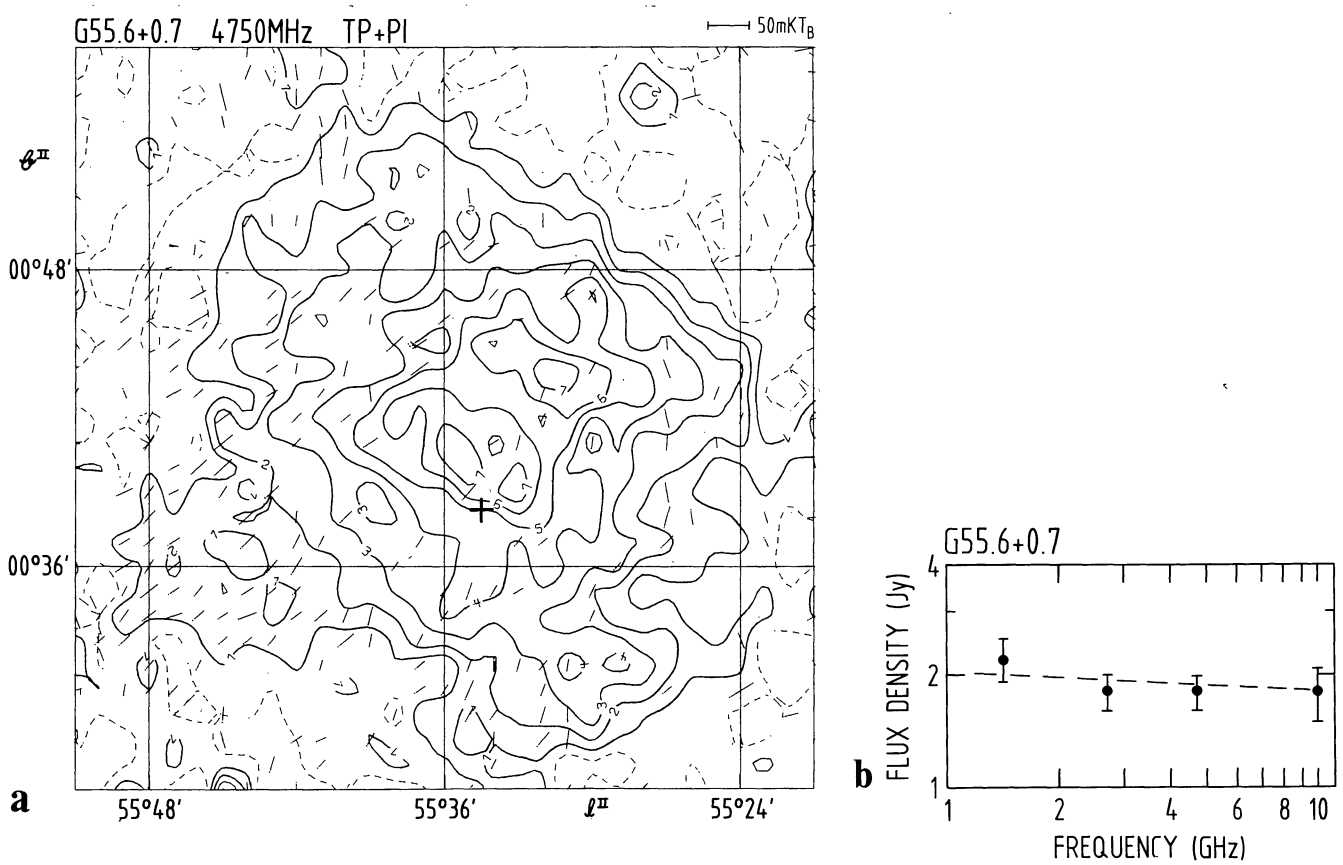

Fig. 6. **a** Contour plot and **b** spectrum of G55.6+0.7. Contour steps are in 20 mK T_B. The HPBW is 2'.4. The r.m.s. noise is about 12 mK T_B in total power and 15 mK T_B in PI. PI is plotted above 20 mK T_B. A cross marks the position of pulsar PSR 1929+20

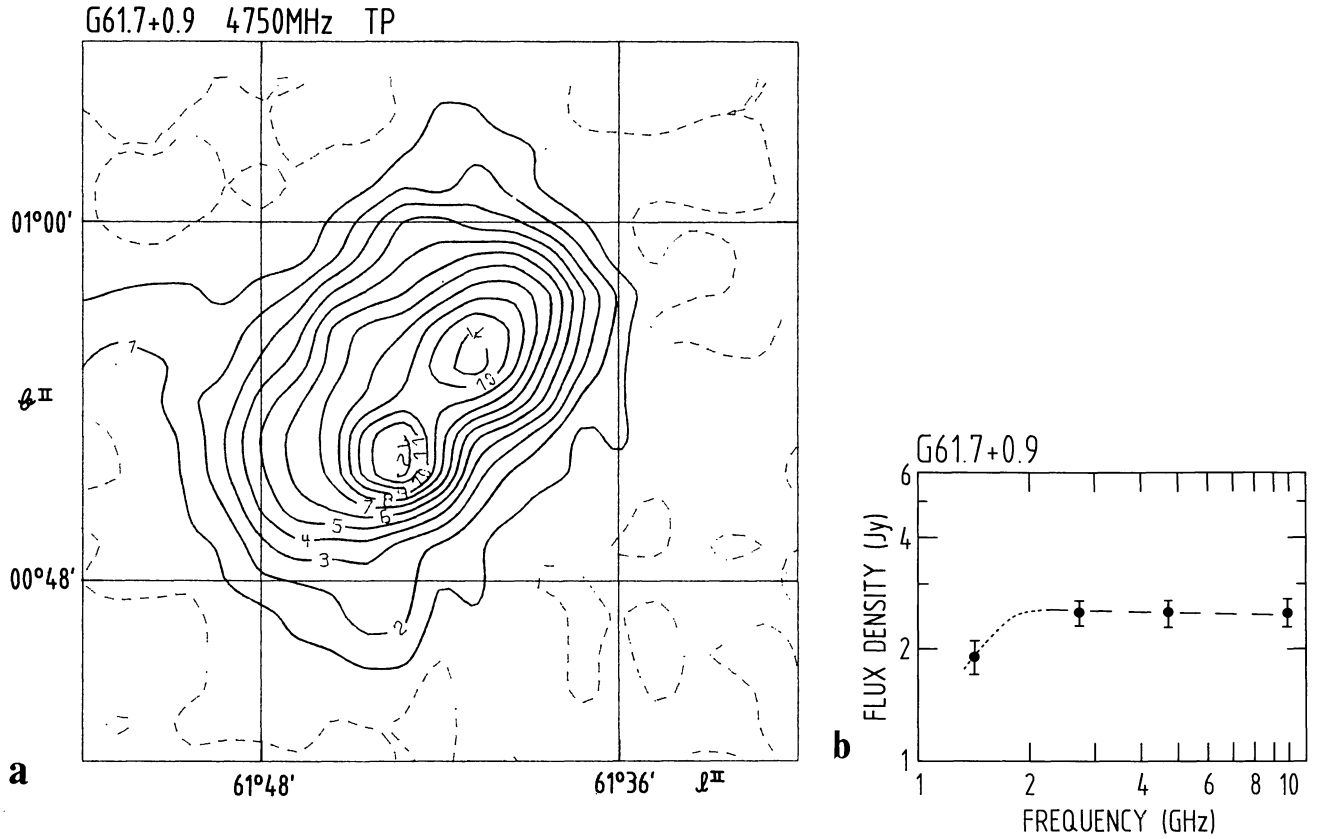

Fig. 7. **a** Contour plot and **b** spectrum of G61.7+0.9. Contour steps are in 40 mK T_B. The HPBW is 2'.4. The r.m.s. noise is about 8 mK T_B in total power

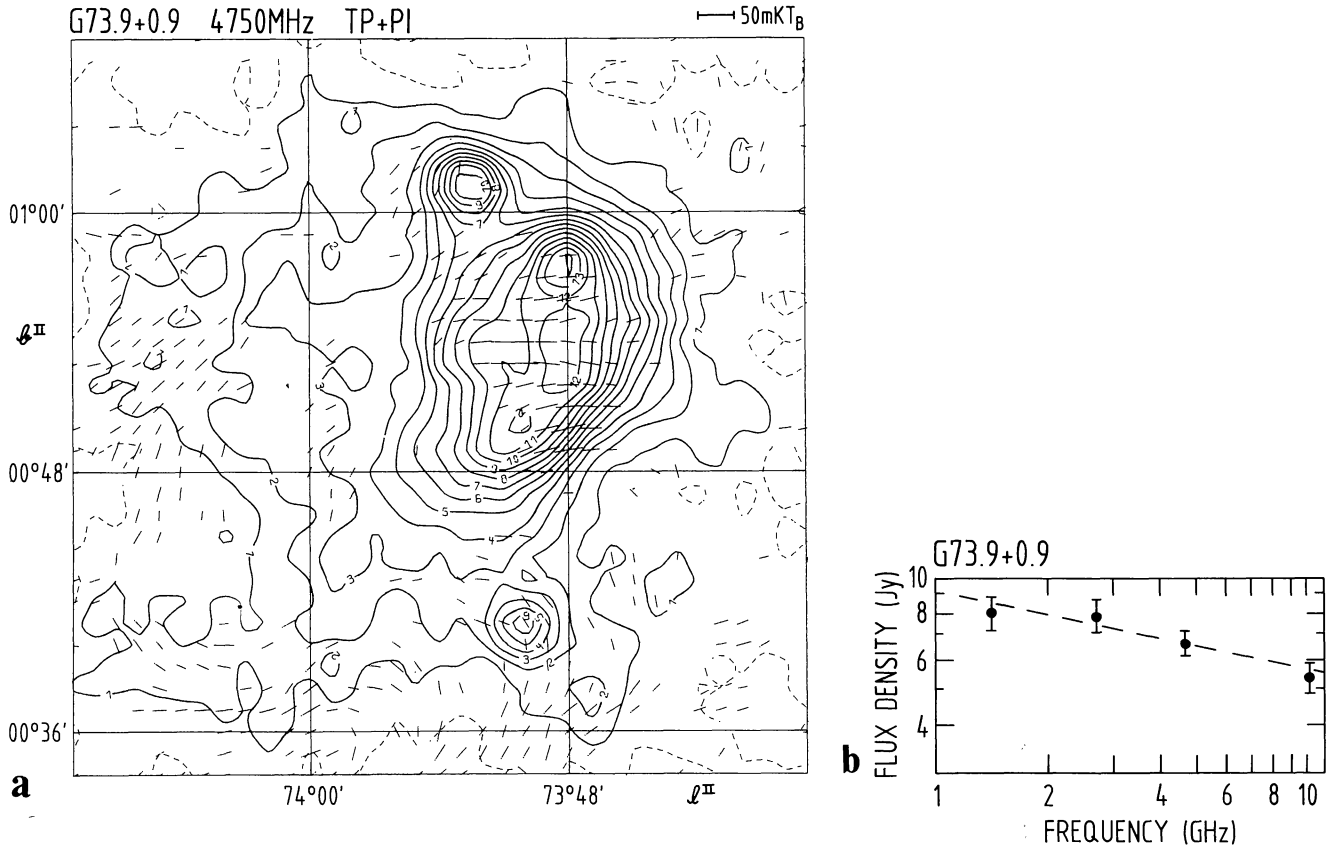

Fig. 8. **a** Contour plot and **b** spectrum of G73.9+0.9. Contour steps are in 40 mK T_B. The HPBW is 2'.4. The r.m.s. noise is about 12 mK T_B in total power and 10 mK T_B in PI. PI is plotted above 20 mK T_B

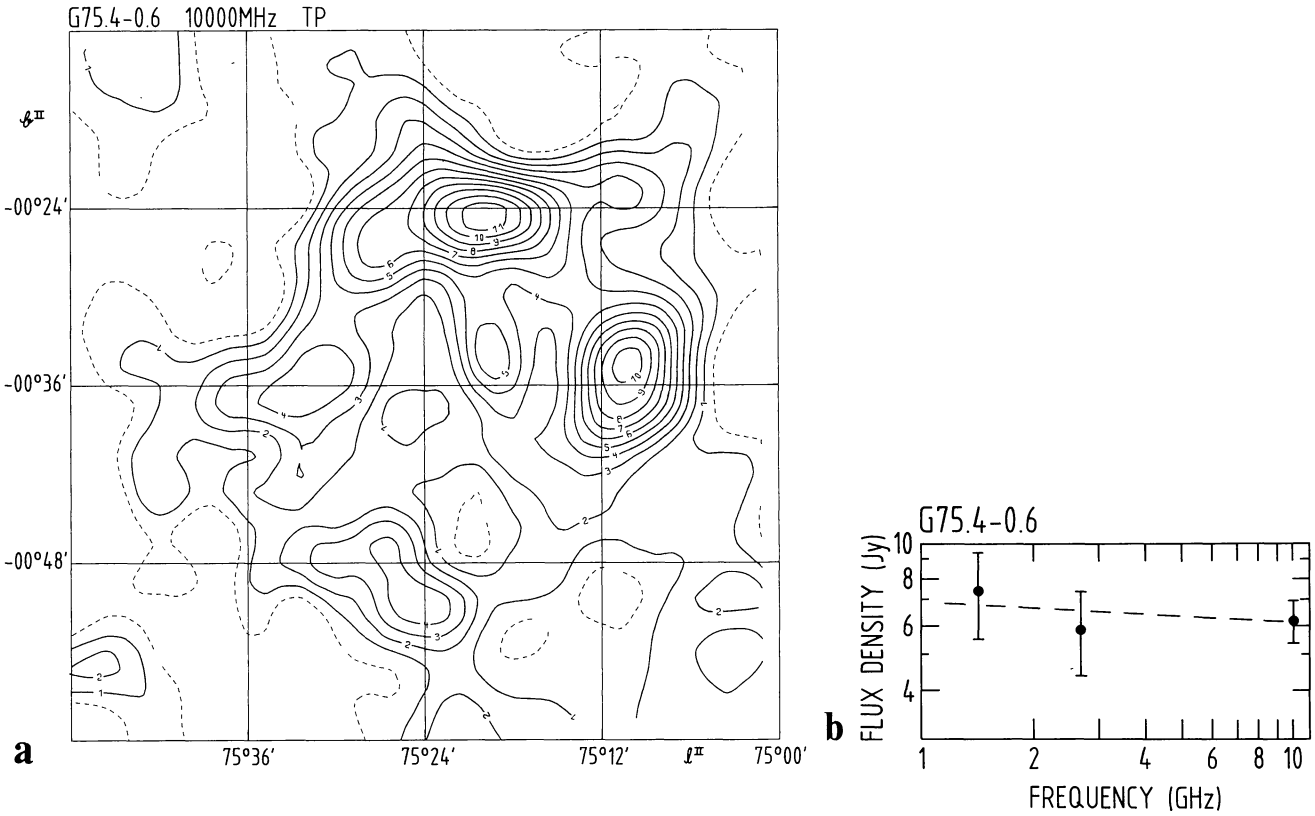

Fig. 9.a Contour plot and **b** spectrum of G75.4−0.6. Contour steps are in 10 mK T_B. The HPBW is 4'.4. The r.m.s. noise is about 4 mK T_B in total power

known, thus a lower limit of the distance to the nonthermal emission cannot be given. The small diameter source at $l=16°56'.8$, $b=-1°2'.2$ (peak flux density ≈ 0.11 Jy at 4750 MHz) coincides with the Wolf-Rayet star IC14−19 of type WN6. The source at $l=16°43'.5$, $b=-1°11'.1$ has a peak flux density of ≈ 0.13 Jy at 4750 MHz.

3.3. G30.7+1.0 ($\alpha_{50}=18^h40^m.2$, $\delta_{50}=-1°35'$)

A high percentage polarization (up to 40%) and a nonthermal spectrum classify this source as a supernova remnant. The type of this SNR is uncertain. There is an indication of a shell in the northwestern part, but the emission is also prominent in the inner part. The spectral index is almost uniform across the source with $\alpha=-0.4$ ($S_\nu \sim \nu^\alpha$), in agreement with shelltype SNR's. The small diameter source at $l=30°44'.7$, $b=1°0'.5$ (peak flux density ≈ 0.1 Jy at 4750 MHz) cannot be distinguished in the spectral index map, it is probably nonthermal with a similar spectral index as G30.7+1.0. The integrated polarization percentage drops from $\approx 30\%$ at 4750 MHz to 3% at 2695 MHz (Junkes, 1985), indicating strong depolarization and large Faraday rotation, which may also cause the complexity on the polarization angle distribution (see Fig. 3a).

3.4. G43.45+0.5 ($\alpha_{50}=19^h6^m.6$, $\delta_{50}=9°30'$)

The integrated spectral index of this object between 1420 MHz and 4750 MHz is flat, while *TT*-plots between 2695 MHz and 4750 MHz give $\alpha=-0.33$. This is an indication of strong background confusion, which can be seen in the 2695 MHz survey maps (Reich et al., 1984a) to be particularly strong in the southern part. There is a slight tendency of the spectrum to steepen from the centre towards north and south, but this may partly be caused by the confusion. At 10 GHz only a part of the sources has been mapped. Hence only a lower limit of the integrated flux density at this frequency can be given. A discrete source is located at the centre, $l=43°25'.7$, $b=0°31'$ (peak flux density 0.14 Jy at 4750 MHz). The spectrum of this source is flat ($\alpha=0\pm0.2$). Whether this object is related to the diffuse emission is unclear. No linear polarization has been detected. The morphology of G43.45+0.5 resembles that of a bent radio galaxy rather than a galactic source. New observations with high angular resolution and an optical identification of the central source are necessary to reveal the true nature of this object.

3.5. G52.0+0.6 ($\alpha_{50}=19^h22^m.8$, $\delta_{50}=17°5'$)

This object is a large complex of about half a degree in size. The spectrum between 2695 MHz and 10 GHz is that of an optically thin thermal source. The spectral index shows very little variation across the source. Even the two discrete sources at the end of the northern ridge show the same spectrum and perhaps belong to the whole complex. No obviously related optical features could be found on the Palomar prints. The discrete source at $l=51°45'.8$, $b=0°47'.9$ (peak flux density of 0.35 Jy at 10 GHz) coincides with an IRAS point source. The small diameter source at $l=52°13'.8$, $b=0°44'.2$ has a peak flux density of 0.68 Jy at 10 GHz. The whole complex resembles the Scutum ring (Handa et al., 1985), an association of an old diffuse H II-shell and newly born stars with compact H II-regions.

3.6. G55.6+0.7 ($\alpha_{50}=19^h29^m.8$, $\delta_{50}=20°17'$)

The pulsar PSR 1929+20 is located close to the centre of the radio emission of this object. The pulsar is at a distance of 5.7 kpc

(Manchester and Taylor, 1981) and the age is estimated to 10^6 years, much older than that of any known supernova remnant. The spectrum of the radio source is flat ($\alpha = 0.0$). No significant polarization could be detected above the sensitivity limit of 5%. Related optical emission on the Palomar prints has not been found. The morphology of G55.6+0.7 and the spectral index agree with a classification as a filled centered SNR or an optically thin H II-region. However, the low polarization percentage argues in favour of an H II-region.

3.7. G61.7+0.9 ($\alpha_{50} = 19^h42^m.1$, $\delta_{50} = 25°41'$)

The morphology of this object suggests an identification as a double extragalactic source. However, the spectrum suggests a thermal source that is optically thin above 2000 MHz. This is unusual for an extragalactic source. Additionally, no linear polarization above the detection limit of 1% has been observed at 4750 MHz. The southern radio peak coincides with an IRAS point source; related optical emission for G61.7+0.9 could not be found on the Palomar prints. Based on the radio data, it is likely that G61.7+0.9 is an H II-region.

3.8. G73.9+0.9 ($\alpha_{50} = 20^h12^m.3$ $\delta_{50} = 36°3'$)

The polarization and the nonthermal spectral index classify this object as a supernova remnant. The source is heavily confused by large scale emission of the Cygnus area (see Reich et al., 1984a). Therefore, a separation of the faint emission of the SNR and of the underlying broad spur-like emission is difficult. The source might be of shell type or of intermediate type (class C, Weiler, 1984). At the highest available angular resolution (2'.4 at 4750 MHz) several discrete sources are visible, the nature of which are not known. The source at $l = 73°52'.7$, $b = 1°1'.3$ (peak flux density 0.12 Jy at 4750 MHz) coincides with an IRAS source. Two other discrete sources are at $l = 73°48'$, $b = 0°57'.5$ (peak flux density 0.1 Jy) and at $l = 73°50'.2$, $b = 0°40'.7$) peak flux density 0.08 Jy). The polarization E-vector indicates a tangential magnetic field in case of low Faraday rotation. However, large Faraday rotation is expected in the direction of the Cygnus region, which is supported by the fact that no polarization has been detected at 2695 MHz (Junkes, 1985). High frequency observations of the polarization are necessary to determine the orientation of the intrinsic magnetic field.

3.9. G75.4−0.6 ($\alpha_{50} = 20^h22^m.6$, $\delta_{50} = 36°26'$)

This object is a ring of optically thin H II-regions with some underlying diffuse probably thermal emission. The spectrum is flat with little variation across the source. It is similar to G52.0+0.6 and the Scutum ring.

4. Summary

Among the nine presented objects five sources could be most likely identified as H II-regions (G7.45+0.7, G52.0+0.6, G55.6+0.7, G61.7+0.9, G75.4−0.6), while two new supernova remnants have been found (G30.7+1.0, G73.9+0.9). G43.5+0.5 appears morphologically as a radio galaxy, however its spectrum is flat. G16.85−1.05 consists of thermal emission of RCW 164 and a strongly polarized component. It is not possible from the present data to separate both components. RCW 164 may be seen in front of the nonthermal emission of a possible supernova remnant.

Acknowledgements. E.F., W.R., and P.R. gratefully thank Prof. Akabane for kind hospitality during their stay at NRO. P.R. thanks Prof. Morimoto for financial support. E.F. and W.R. are grateful to the Alexander von Humboldt Stiftung for travel grants.

References

Fürst, E., Reich, W., Reich, P., Sofue, Y., Handa, T.: 1985, *Nature* **314,** 720
Handa, T., Sofue, Y., Reich, W., Fürst, E., Suwa, I., Fukui, Y.: 1985, *Publ. Astron. Soc. Japan* (submitted)
Haslam, C.G.T.: 1974, *Astron. Astrophys. Suppl.* **15,** 333
Henbest, N., Knapp, W.: 1984, *Bild der Wissenschaft* **4,** 38
Junkes, N.: 1985, Diploma thesis, Bonn University
Kallas, E., Reich, W.: 1980, *Astron. Astrophys. Suppl.* **42,** 227
Manchester, R.N., Taylor, J.H.: 1981, *Astron. J.* **86,** 1953
Reich, W.: 1984, *Kleinheubacher Berichte* **26,** 183
Reich, W., Fürst, E.: 1984, *Astron. Astrophys. Suppl.* **57,** 165
Reich, W., Fürst, E., Steffen, P., Reif, K., Haslam, C.G.T.: 1984a, *Astron. Astrophys. Suppl.* **58,** 197
Reich, W., Fürst, E., Sofue, Y.: 1984b, *Astron. Astrophys.* **133,** L4
Reich, W. et al.: 1986 (in preparation)
Rodgers, A.W., Campbell, C.T., Whiteoak, J.B.: 1960, *Monthly Notices Roy. Astron. Soc.* **121,** 103
Seiradakis, J.H., Reich, W., Sieber, W., Kühr, H., Schlickeiser, R.: 1985, *Astron. Astrophys.* **143,** 471
Sharpless, S.: 1959, *Astrophys. J. Suppl.* **4,** 257
Sofue, Y., Hirabayashi, H., Akabane, K., Inoue, M., Handa, T., Nakai, N.: 1984, *Publ. Astron. Soc. Japan* **36,** 287
Weiler, K.W.: 1984, in *Supernova Remnants and their X-ray Emission, IAU Symp. No.* **101,** eds. I. Danziger, P. Gorenstein, D. Reidel, Dordrecht, p. 299
Wielebinski, R.: 1984, in *Indirect Imaging* ed. J.A. Roberts, Cambridge University Press, p. 199